Autonomous Soaring for Improved Endurance of a Small Uninhabited Air Vehicle

Michael J. Allen*
NASA Dryden Flight Research Center, Edwards, California, 93523-0273, U.S.A.

A relatively unexplored method to improve the endurance of an autonomous aircraft is to use buoyant plumes of air found in the lower atmosphere called *thermals* or *updrafts*. Glider pilots and birds commonly use updrafts to improve range, endurance, or cross-country speed. This report presents a quantitative analysis of a small electric-powered uninhabited air vehicle using updrafts to extend its endurance over a target location. A three-degree-of-freedom simulation of the uninhabited air vehicle was used to determine the yearly effect of updrafts on performance. Surface radiation and rawinsonde balloon measurements taken at Desert Rock, Nevada, were used to determine updraft size, strength, spacing, shape, and maximum height for the simulation. A fixed-width spiral path was used to search for updrafts at the same time as maintaining line-of-sight to the surface target position. Power was used only when the aircraft was flying at the lower-altitude limit in search of updrafts. Results show that an uninhabited air vehicle with a nominal endurance of 2 hours can fly a maximum of 14 hours using updrafts during the summer and a maximum of 8 hours during the winter. The performance benefit and the chance of finding updrafts both depend on what time of day the uninhabited air vehicle is launched. Good endurance and probability of finding updrafts during the year was obtained when the uninhabited air vehicle was launched 30 percent into the daylight hours after sunrise each day. Yearly average endurance was found to be 8.6 hours with these launch times.

Nomenclature

a	=	spiral path constant
A_y	=	aircraft lateral acceleration, m/s^2
b	=	spiral offset from origin, m
C_p	=	specific heat of dry air, °K*m^2/s^2
D	=	aircraft drag force, *N*
Dia	=	updraft diameter, m
DOF	=	degree-of-freedom
g	=	gravitational constant, m/s^2
L	=	aircraft lift force, *N*
Le	=	length of flightpath, m
N	=	number of thermals encountered along a straight line
N_z	=	aircraft normal acceleration, *g*'s
NOAA	=	National Oceanic and Atmospheric Administration
P	=	pressure, mb
P_O	=	reference pressure, mb
Q_G	=	latent heat into ground, *W*/m^2
$\tilde{Q}_H$	=	sensible heat flux, *W*/m^2
Q_H	=	kinematic sensible heat flux, °K*m/s
Q_{OV}	=	surface virtual potential temperature flux, *W*/m^2
Q_S	=	net radiation at surface, *W*/m^2
r	=	radius from target location, m
S_i	=	UAV sink rate, m/s

* Aerospace Engineer, Controls and Dynamics Branch, P.O. Box 273/MS-4840D, Member.

SURFRAD = Surface Radiation
UAV = uninhabited air vehicle
V = aircraft velocity, m/s
W = climb rate, m/s
w_E = environment sink velocity, m/s
w_s = mixing ratio, kg/kg
w_T = updraft velocity, m/s
w^* = free-convective velocity scale, m/s
X_a = length of test area, m
Y_a = width of test area, m
z = aircraft altitude, m
z_i = convective mixing layer thickness, m
β = Bowen ratio, unitless
Γ_D = dry adiabatic lapse rate, °C/m
θ_O = daily average surface potential temperature, °K
ρ = air density, kg/m^3
ϕ = aircraft bank angle, rad
ψ = spiral heading angle, rad

I. Introduction

MANY strategies for extracting energy from updrafts and other atmospheric energy sources have been published.[1-3] These strategies generally give additional insight into the mechanics of soaring flight for glider pilots. Autonomous soaring for uninhabited air vehicles (UAVs) is an emerging field of research. Boslough[4] developed a simulation environment for a UAV to mimic and optimize the dynamic soaring maneuvers flown by albatrosses. Flight tests were done to prove the concept, but autonomous dynamic soaring was never attempted. Wharington[5] first proposed autonomous soaring UAVs in 1998 as a method to extend UAV performance and possibly to enable perpetual flight. Optimal guidance algorithms were developed using reinforcement learning and a neural-based thermal locator to autonomously detect and utilize updrafts. Results showed that both simple heuristics and reinforcement learning could be used along with the thermal locator to improve UAV performance; however, the reinforcement learning algorithms were too computationally intensive for real-time use.

The research presented in this report uses the assumption that a sufficient updraft locator and guidance method exist so that simple performance calculations can be made without having to simulate the aircraft guidance and control system. This report uses measured meteorological data with a simple 3-degree-of-freedom (DOF) simulation of a UAV to quantify the increase in endurance as a result of autonomous soaring for a small UAV. Derivation of an updraft model from surface and rawinsonde balloon measurements taken at Desert Rock, Nevada (lat. 36.63 deg N, long. 116.02 deg W, elev. 1007 m), is given as well as results of this research showing significant endurance improvements.

II. Convective-Layer Scale Factors

The convective layer is the lowest region of the atmosphere where significant mixing occurs. During calm conditions, buoyant plumes of air that have been heated at the surface cause local mixing. These plumes of air, called *updrafts* or *thermals*, can be parameterized with convective scale factors. Convective scale factors were calculated from measured data and then used to determine atmospheric conditions for the UAV simulation.

Measurements from the National Oceanic and Atmospheric Administration (NOAA) Surface Radiation (SURFRAD) station in Desert Rock, Nevada, were used to calculate convective-layer scaling parameters. SURFRAD instrumentation includes a radiometer platform, meteorology tower, and solar tracker. Measurements were taken every 3 min. A rawinsonde station is also collocated with the SURFRAD site where rawinsonde balloons were launched every 12 hr. Surface temperature, wind, and radiation measurements along with balloon-measured temperature and humidity from the entire year of 2002 were collected and used in this study.[6] Each simulation step was tied to an actual time in the measured data so that UAV simulation results would reflect actual conditions during each day of 2002. The appendix gives the equations used to calculate convective-layer scaling parameters from measured data.

III. Updraft Calculations

The convective-layer scale parameters, w^* and z_i, were calculated using equations given in the appendix. Calculations were made at each simulation time step and were used to determine the updraft velocity, diameter, and spacing. The calculations given in this report determine the updraft velocity, size, and spacing that the UAV will encounter at a given altitude. Updraft velocity was calculated using Eq. (1) taken from Ref. 7.

$$w_T = w^* \left(\frac{z}{z_i}\right)^{\frac{1}{3}} \left(1 - 1.1\frac{z}{z_i}\right) \tag{1}$$

Equation (1) was solved using the aircraft altitude, z, and the scale parameters, w^* and z_i, from surface measurements.

Maximum updraft velocity in Eq. (1) occurs at an altitude ratio, z/z_i, of approximately 0.25. This indicates that UAV climb rate in an updraft will likely peak at $0.25z/z_i$ and slowly taper to zero as altitude increases. High altitude updrafts are characterized by reduced strength and increased diameter. Updraft diameter increases exponentially with increasing altitude as given by Eq. (2).

$$Dia = 0.203\left(\frac{z}{z_i}\right)^{\frac{1}{3}} \left(1 - 0.25\frac{z}{z_i}\right) * z_i \tag{2}$$

This equation defines the thermal size to be nearly zero at the surface and have a maximum diameter when $z = z_i$. Low altitude updrafts are not likely to be well-predicted by Eq. (2). This factor is remedied by enforcing a lower-altitude limitation on the UAV that is discussed in the simulation section.

Equation (3) gives the number of updrafts encountered for a given straight-line flight-path distance.[7]

$$N = 1.2\frac{Le}{z_i} \tag{3}$$

In Eq. (3), N is the number of thermals and Le is the length of the flightpath. The fixed ratio of 1.2 was chosen from the data presented in Ref. 7 to conservatively represent all altitudes in a simulation that do not allow updraft dissipation or merging. This seems to be a good technique since most dissipation and merging occur in the surface layer, defined as $z \leq 0.1z_i$. Equation (3) can be used to determine the number of updrafts for a given area of length X_a and width Y_a and a given updraft diameter. This relationship is given in Eq. (4).

$$N = \frac{1.2 * Y_a * X_a}{z_i * Dia} \tag{4}$$

Updraft positions were randomly chosen and held for 20 min at a time. The 20-min thermal lifespan was chosen from estimates given in the literature[2,8] and from personal observation of cumulus clouds. Overlapping updrafts were ignored so that the UAV only experienced the effects of one updraft at a time. Figure 1 shows a typical summer updraft field. The maximum diameter of these updrafts, taken at $z = z_i$ = 3710 m, is 567 m. This diameter falls within the range of updraft diameters measured by Konovalov from flight.[9]

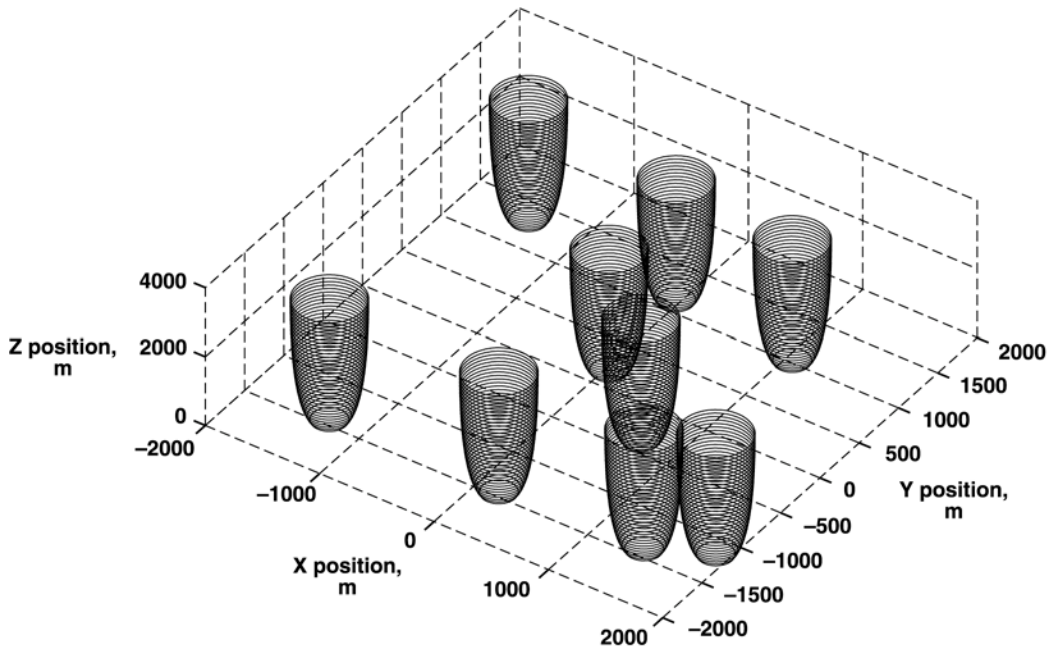

Figure 1. Typical summer updraft field.

The downward air velocity was calculated for the environment outside of the updrafts by assuming conservation of mass. Equation (5) gives the environment sink velocity.

$$w_E = \frac{-N * \pi * \left(\frac{Dia}{2}\right)^2 * w_T}{Y_a * X_a - N * \pi * \left(\frac{Dia}{2}\right)^2} \tag{5}$$

This velocity was applied to all areas outside of the updrafts. The use of constant environment velocity between updrafts seems to better reflect flight measurements[7] as opposed to "hat" updraft distributions that surround each updraft with a ring of downward moving air.

IV. Simulation

A 3-DOF simulation was constructed to determine the yearly benefit of using updrafts to extend UAV endurance during a surveillance mission. For this mission, the UAV must stay above 200 m and remain inside the cone airspace boundary given in Fig. 2. This type of boundary was chosen because it ensures that the vehicle will always have line of sight to the target area. Restrictions on upper altitude were not used here but are addressed later in the results section. These boundaries were used to represent a surveillance mission where the UAV is used to monitor a target location or area for as long as possible.

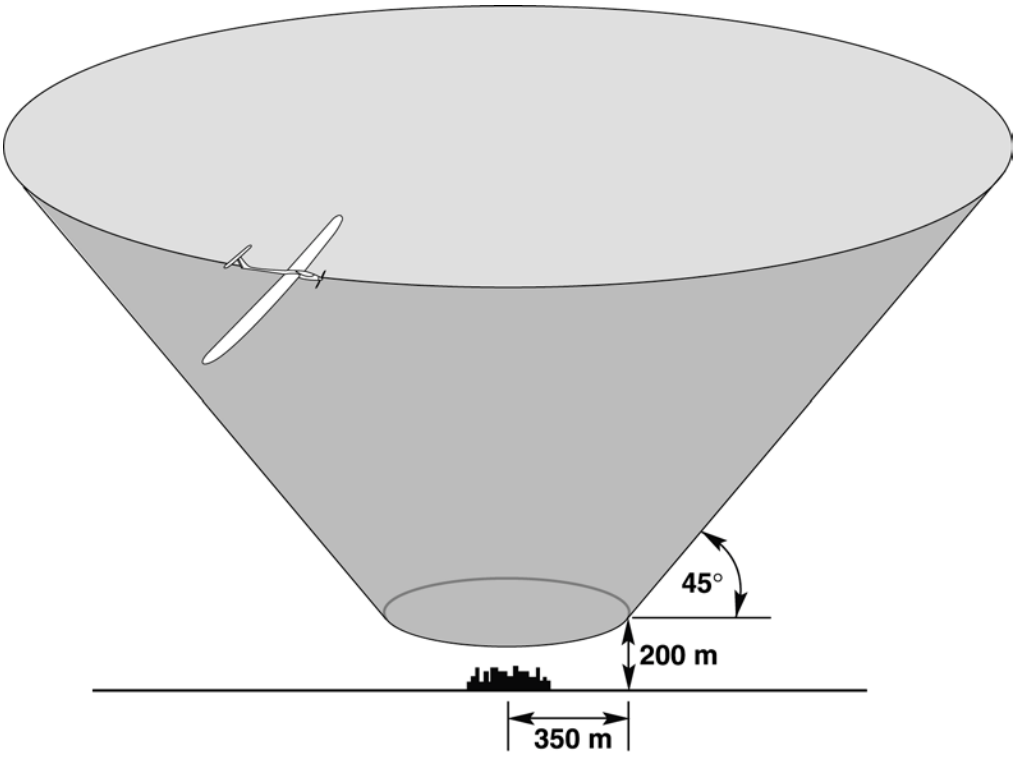

Figure 2. Mission airspace cone boundary.

The performance of the aircraft was derived from flight measurements of a 4.3-m span radio-control cross-country glider[10] and published UAV data.[11] A two-hr nominal-powered flight endurance was chosen to provide a baseline for this study. Current electric-powered UAVs of this size have endurances ranging from 45 min to 2 hr.[12] Table 1 gives aircraft performance and other simulation settings.

Table 1. Simulation settings.

Parameter	Value
Aircraft velocity	12 m/s
Sink speed	0.531 m/s
Nominal endurance	2 hr
Updraft lifespan	20 min
Simulation step time	5 s
Centering time penalty	30 s
Altitude floor	200 m

An Archimedes spiral pattern was chosen for the UAV to fly while searching for updrafts. The spiral, given in Eq. (6), allows the UAV to cover a given circular area without crossing the same point twice.

$$r = a * \psi + b \tag{6}$$

Equation (6) defines a radius, r, from the target location for every spiral heading angle, ψ, given a spiral of width, $2\pi a$, and offset, b, from the origin.[13] This equation was solved for each point along the flightpath with the constraint that aircraft velocity remained constant. Updraft detection was done with aircraft response only. An assumption was made that the UAV uses measured aircraft accelerations and pressure-altitude changes to detect

updrafts. This method was shown to be feasible by Wharington.[14] To find an updraft, the UAV must fly a search pattern until an updraft is encountered.

Once an updraft was encountered, the UAV altitude was held for 30 s to account for updraft detection and centering. The 30-s time penalty was put on the simulation to account for the time that an actual vehicle would spend detecting and engaging an updraft. Thirty seconds was chosen because it is more than adequate for the pilot of a model or full-size glider to detect and center an updraft. After detection, the UAV flew in a circular ground track that was centered at the updraft location. The ground track did not include the effects of horizontal wind in this simulation. An assumption was made that the updraft detection and centering control design will be able to account for the movement of updrafts caused by wind. Glider pilots typically are able to find updrafts in light to moderate wind. To ensure that high-wind updrafts were not used, a wind limit of 12.8 m/s was enforced. During circling flight, lateral acceleration was calculated using Eq. (7).

$$A_y = \frac{V^2}{0.8 * \frac{Dia}{2}} \tag{7}$$

Lateral acceleration was used to calculate bank angle, ϕ, using Eq. (8) and normal acceleration, N_z, using Eq. (9).

$$\phi = \tan^{-1}\left(\frac{A_y}{9.81}\right) \tag{8}$$

$$N_z = \frac{1}{\cos(\phi)} \tag{9}$$

The sink rate of the UAV was adjusted for bank angle using Eq. (10) from Ref. 14. These equations ensure that small, weak updrafts that require high-bank angle circling will not be used. The maximum bank angle for all simulation runs was found to be 39 deg.

$$S_i = \frac{V * \left(1 + N_z^2\right)}{2 * \frac{L}{D}} \tag{10}$$

Climb rate, W, was obtained by subtracting S_i from w_T given in Eq. (1). The UAV remained in each updraft until the climb rate became negative or the updraft duration was exceeded. The UAV entered an unpowered thermal seek mode immediately after leaving an updraft. Power was only used when the UAV was at the altitude floor of 200 m. The sink rate used during the unpowered thermal seek mode was the sum of the environment sink velocity, W_E, and UAV sink rate, S_i, with $N_z = 1$.

V. Results

Simulation results revealed that the UAV was able to use updrafts year-round and during a large part of the day to extend its duration. Figure 3 gives a typical plot of the aircraft position. The UAV generally found an updraft early in the flight and remained above the altitude floor until the afternoon when the sun angle was reduced. Figure 4 gives the height-above-ground time histories for typical winter, spring, summer, and fall flights. The UAV flew in a relatively narrow altitude range in the winter and was able to fly most of the day without power. Summer time histories show much greater altitude variations as well as greater endurance.

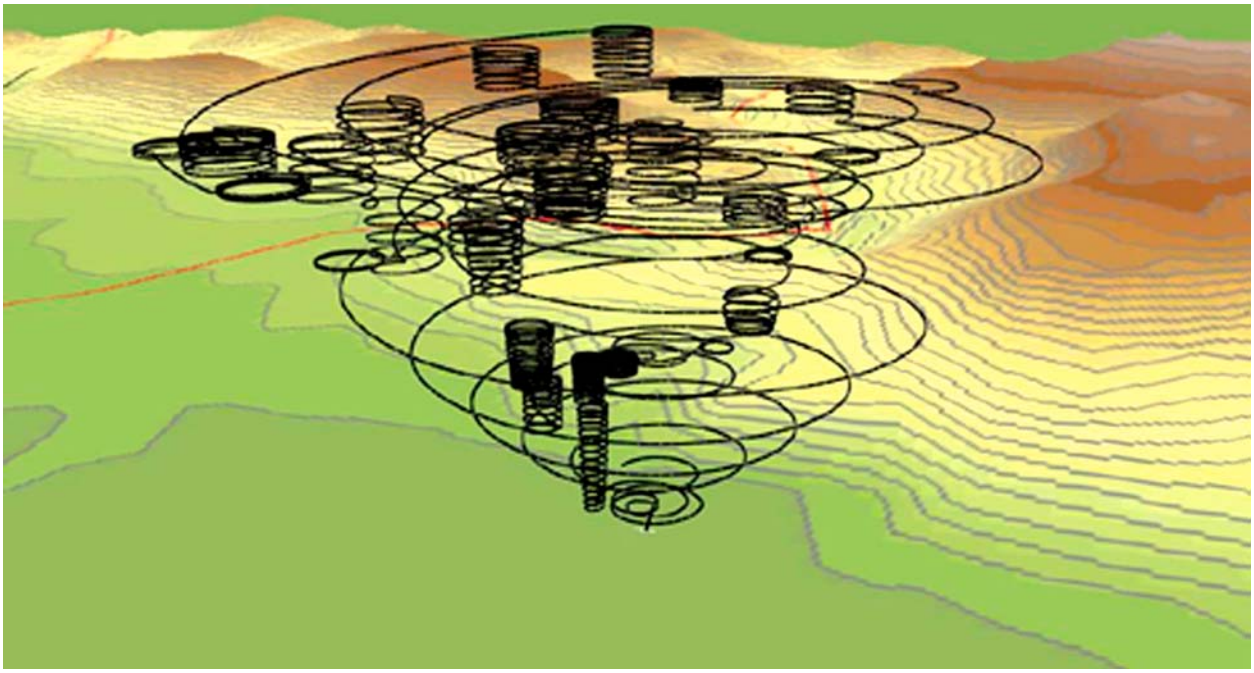

Figure 3. Typical flightpath.

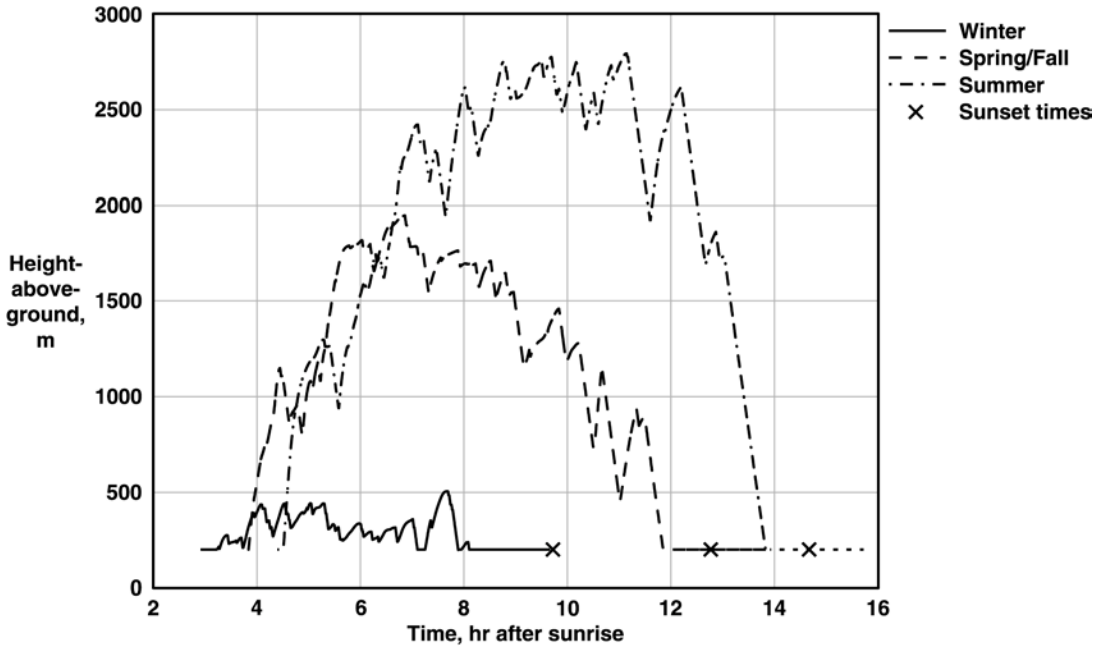

Figure 4. Typical UAV height-above-ground time histories.

Endurance benefit was found to vary with season and daily launch time. An early morning launch could cause the UAV to consume its battery life before the updrafts became usable later in the day. A late launch could cause the UAV to miss most of the usable updrafts that occur in the morning. Multiple launch times were tested during this study. Launch times are given in fractions of daylight hours to account for varying day lengths during the year. A launch time of 50 percent indicates that the aircraft was launched at the middle of each day. Figure 5 gives results from these studies, showing the UAV endurance for each day with varied launch times. Sinusoidal trends in endurance are because of season whereas scatter about the trend is caused by daily variations. Maximum endurances

were obtained with a launch time of 15 percent for all times of the year. The maximum summer endurance is over 14 hr using only 2 hr of battery power. Although maximum benefit is obtained with an early launch, the risk associated with early launch times is that the UAV will exhaust its power and be forced to land before thermal convection picks up in the late morning. Figure 6 shows the calculated probability of successful use of updrafts to extend duration during the year for various launch times. Probabilities were calculated using a 30-day-wide sliding window. Early and late launch times have a reduced probability of success because of the reduced ground temperatures during those times. Overall, a launch time of 30 percent gave good performance and probability of success.

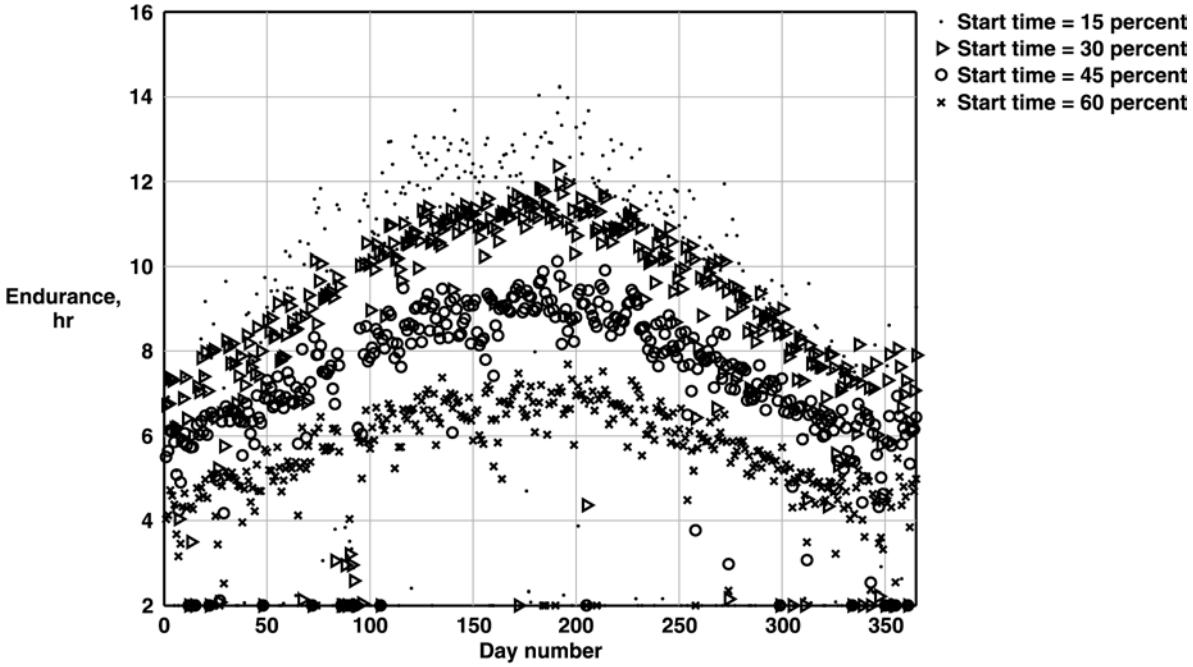

Figure 5. Endurance multiple for each day using various launch times.

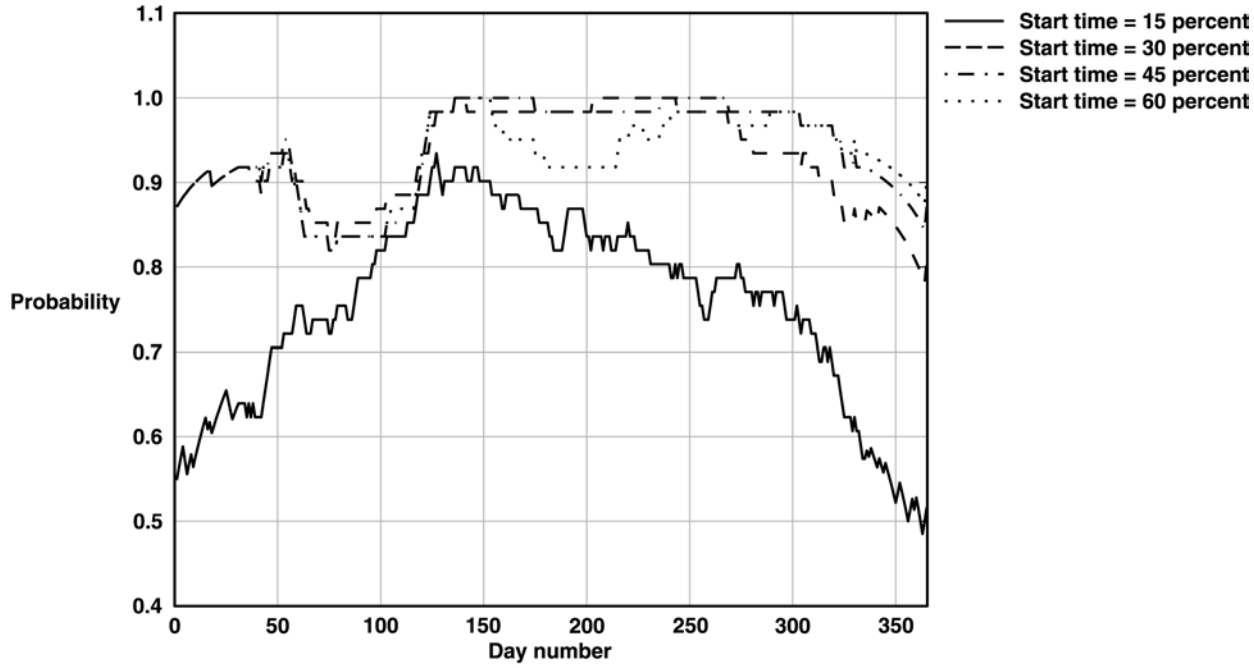

Figure 6. Probability of obtaining endurance increase using various launch times.

Power consumption of non-thrust related devices such as avionics, actuators, and payload was not considered. These devices differ widely in power usage and will require serious consideration during extended duration flights. One method of generating power for these devices is called *regenerative soaring*. Regenerative soaring uses the propeller-motor combination on the aircraft as a wind turbine to convert altitude gained from updrafts into electricity. MacCready proposed that this technique could be used by small UAVs to make long duration flights.[15] Feasibility studies using the simulation described here have shown that regenerative soaring does not produce as much power as solar panels but may be easier and less costly to implement.

Sensitivity studies were conducted to determine the relationship between key simulation parameters and the yearly average endurance. Table 2 lists the results of these studies. The solution is insensitive to many key simulation parameters, indicating that autonomous soaring may apply to other aircraft and other locations. Aircraft sink rate has a large effect on soaring performance because aircraft sink rate is used to determine the aircraft climb rate for a given updraft velocity and it determines the time available to search for updrafts during the descent. An unexpected result from this study is that the yearly average endurance is relatively insensitive to the number of updrafts in a given area and is insensitive to the lifespan of the updrafts. One explanation for these results is that updrafts of sufficient strength that the UAV will use are easily located.

Table 2. Sensitivity study results.

Parameter	Value	Perturbation, percent	Yearly average endurance, hr	Change in endurance, percent
L/D	15.8	–30	8.63	+0.17
L/D	29.4	+30	8.54	–0.83
Sink velocity	–0.37 m/s	–30	9.27	+7.58
Sink velocity	–0.69 m/s	+30	7.91	–8.10
N	calculated	–30	8.47	–1.69
N	calculated	+30	8.67	+0.67
Updraft lifespan	14 min	–30	8.56	–0.61
Updraft lifespan	26 min	+30	8.63	+0.17
w_T	calculated	–30	7.96	–7.62
w_T	calculated	+30	8.92	+3.60
z_i	calculated	–30	8.20	–4.75
z_i	calculated	+30	8.92	+3.53

Constraints on the upper altitude of the airspace shown in Fig. 2 were not used in this study. To investigate the sensitivity of upper altitude limitation on performance, the simulation was also run with varying constraints on maximum allowable altitude. UAV sensor payloads may dictate upper altitude limitations for this class of vehicle. Figure 7 shows the results from this study. Significant performance can be obtained even with highly restrictive altitude limits. A yearly average endurance of more than 5 hr was obtained with height-above-ground tightly restricted to remain between 200 m and 300 m.

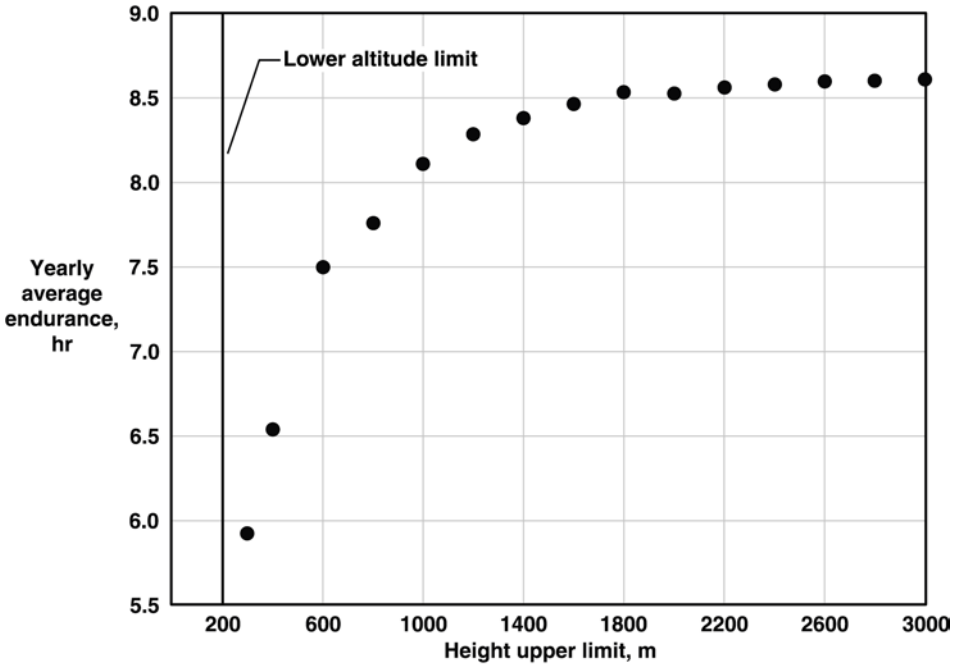

Figure 7. Change in endurance due to height-above-ground limit. Lower height limit is 200 m.

VI. Application of Results to Other Locations

The results of this study give a UAV performance benefit prediction at Desert Rock, Nevada. This location is very conductive to updraft formation; however, other locations, topography, and terrain are still conductive to soaring because convection requires little more than surface heating. The number of soaring birds and aircraft found around the globe evidences the wide range of favorable soaring conditions. The routine use of updrafts by migrating birds can be found in numerous literature.[16-19] Migrating birds are known to vary their route considerably to remain in regions of atmospheric lift. Measurements of the flightpaths of frigatebirds show that they soar in updrafts both day and night above the tropical waters of Guiana, and migrating hawks soar in updrafts during every season of the year. Piloted gliders have performed exceptional flights of duration and distance using atmospheric energy alone. Gliders are flown for recreation in nearly every continent and in every season.

VII. Conclusions

Updraft parameters were calculated from surface measurements and used in a simple three-degree-of-freedom simulation to replicate autonomous soaring in updrafts. Using this simulation with the given uninhabited air vehicle performance parameters, the following conclusions were made.

1) The use of convective lift in the atmosphere can give a 12 hour increase in endurance of a small electric-powered uninhabited air vehicle with a nominal endurance of 2 hours.
2) Performance increases can be obtained during any season of the year and during the majority of daylight hours.
3) The overall performance increase has a low sensitivity to many key simulation parameters including: aircraft glide slope, number of updrafts, updraft lifespan, updraft velocity, and height-above-ground upper limit.

Appendix: Convective-Layer Scale Calculations

Convective-layer scale calculations were used to reduce measured surface and balloon data into a usable form. Updraft velocity, size, shape, and spacing can be calculated from the convective-layer scale factors given in these equations.

The convective-layer thickness, z_i, is the maximum height-above-ground that updrafts generally obtain. The mixing layer thickness was calculated using predawn rawinsonde balloon data and measured surface temperatures. Each measured surface temperature was used to determine z_i by intersecting the balloon-measured temperature profile with the surface temperature using the dry adiabatic lapse rate (Γ_D) of 0.00975 °C/m. Figure A-1 shows an example of the z_i calculation.

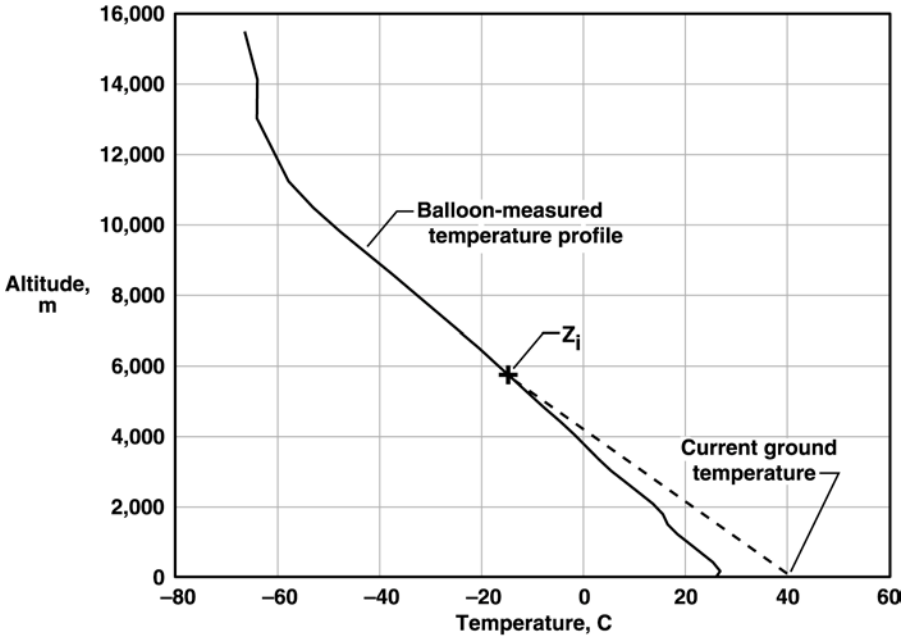

Figure A-1. Example of z_i calculation.

A surface heat budget was used to calculate the free-convection scaling velocity, w^*. The first step in this process is to calculate the sensible heat flux using an equation found in Ref. 8.

$$\tilde{Q}_H = \frac{\beta(-Q_S + Q_G)}{(1+\beta)} \tag{A-1}$$

In this equation, $\tilde{Q}_H$ is the sensible heat flux, Q_S is the net radiation at the surface, Q_G is the latent heat into the ground, and β is the Bowen ratio, defined as the ratio of sensible to latent heat fluxes at the surface. A Bowen ratio of 5, chosen from Ref. 8, was used in this study. The net radiation was measured directly by the SURFRAD station and Q_G was calculated using Eq. (A-2).

$$Q_G = 0.1 * Q_S \tag{A-2}$$

Sensible heat flux was then converted to its kinematic form using Eq. (A-3).

$$Q_H = \frac{\tilde{Q}_H}{\rho * C_p} \tag{A-3}$$

The surface virtual potential temperature flux, Q_{OV}, was then calculated with Eq. (A-4)

$$Q_{OV} = Q_H\left(1 + 0.61 * w_s\right) \tag{A-4}$$

using the mixing ratio, w_s, calculated from surface measurements. Equations (A-1-A-4) determine the surface heat budget required to calculate Q_{OV}. The convective scaling velocity was then calculated using Eq. (A-5):

$$w^* = \left(Q_{OV} * z_i * \frac{g}{\theta_O}\right)^{\frac{1}{3}} \tag{A-5}$$

where g is the gravitational constant and θ_O is the daily average surface potential temperature given by Eq. (A-6).

$$\theta_O = \overline{T}\left(\frac{P_O}{P}\right)^{.286} \tag{A-6}$$

Equation (A-6) was solved using the average measured surface temperature ($\overline{T}$) and pressure (P) with a reference pressure (P_O) of 1000 mb. The free-convective scaling velocity, w^*, was used to calculate the updraft velocity for a given SURFRAD measurement set. The scaling velocity was set to zero if the surface wind velocity was greater than 25 knots to account for the disruptive effect of high winds on updrafts.

References

[1]Reichmann, H., "Cross Country Soaring," Soaring Society of America, Inc., 1993, ISBN 1-883813-01-8.

[2]Pagen, D., *Understanding the Sky*, Sport Aviation Pubns, February 1992.

[3]Metzger, D. E., and Hedrick, J. K., "Optimal Flight Paths for Soaring Flight," AIAA-74-1001, *AIAA/MIT/SSA 2nd International Symposium on the Technology and Science of Low Speed and Motorless Flight*, Cambridge, Massachusetts, September 11-13, 1974.

[4]Boslough, M. B. E., "Autonomous Dynamic Soaring Platform for Distributed Mobile Sensor Arrays," SAND2002-1896, Sandia National Laboratories, June 2002.

[5]Wharington, J., and Herszberg, I., "Control of a High Endurance Unmanned Air Vehicle," ICAS-98-3.7.1, AIAA-A98-31555, *21st ICAS Congress*, Melbourne, Australia, September 13-18, 1998.

[6]"The SURFRAD Network," National Oceanic and Atmospheric Administration, URL: http://www.srrb.noaa.gov/surfrad/index.html [cited 27 September 2004].

[7]Lenschow, D. H., and Stephens, P. L., "The Role of Thermals in the Convective Boundary Layer," *Boundary-Layer Meteorology*, 19, 1980, pp. 509-532.

[8]Stull, R. B., *An Introduction to Boundary Layer Meteorology*, Kluwer Academic Publishers, Norwell, Massachusetts, 1988, ISBN 90-277-2769-4.

[9]Konovalov, D. A., "On the Structure of Thermals," *12th OSTIV Congress,* Alpine, USA, 1970.

[10]Ellias, J., "Performance Testing of RNR's SBXC Using GPS," Camarillo, California, URL: http://www.xcsoaring.com/articles/john_ellias_1/sbxc_performance_test.pdf.

[11]Dornheim, M. A., "Get Me Through the Night," *Aviation Week & Space Technology,* September 15, 2003, pp. 66-70.

[12]"Unmanned Aerial Vehicles and Drones," *Aviation Week & Space Technology*, January 19, 2004, pp. 112-119.

[13]Peressini, A. L., et al., "Precalculus and Discrete Mathematics," Scott, Foresman and Company, Glenview, Illinois, 1992, ISBN 0-673-33366-3.

[14]Wharington, J., "Autonomous Control of Soaring Aircraft by Reinforcement Learning," PhD Thesis, Royal Melbourne Institute of Technology, Melbourne, Australia, November 1998.

[15]MacCready, P. B., "Regenerative Battery-Augmented Soaring," *Self-Launching Sailplane Symposium*, National Soaring Museum, Elmira, New York, July 16, 1998.

[16]Shamoun-Baranes, J., et al., "Differential Use of Thermal Convection by Soaring Birds Over Central Israel," *The Condor*, 105:208-218, The Cooper Ornithological Society, Vol. 2, May 2003, pp. 208-218.

[17]Weimerskirch, H., et al., "Frigatebirds Ride High on Thermals," *Nature*, Vol. 421, January 23, 2003, pp. 333-334.

[18]Kerlinger, P., "Flight Strategies of Migrating Hawks," The University of Chicago Press, 1989, ISBN 0-226-43167-3.

[19]Pennycuick, C. J., "Bird Flight Performance A Practical Calculation Manual," Oxford University Press, New York, 1989, ISBN 0-19-857721-4.